Volume 1
Number 4
July 2020
Pages 497–928

Materials Advances

rsc.li/materials-advances

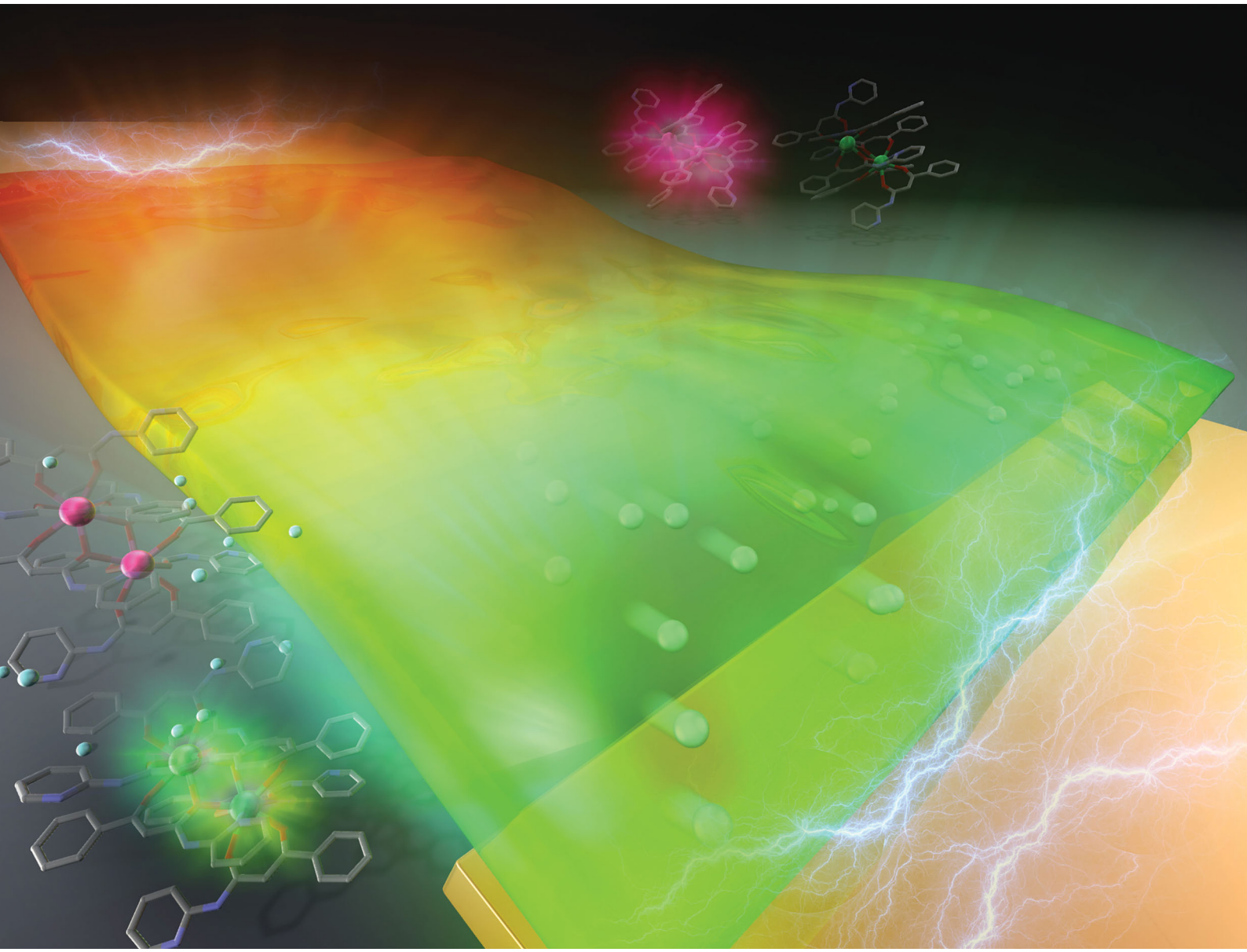

ISSN 2633-5409

ROYAL SOCIETY OF CHEMISTRY

COMMUNICATION

Hajime Kamebuchi, Makoto Tadokoro *et al.*
Development of tuneable green-to-red emitting transparent film based on Nafion with Tb^{III}/Eu^{III} β-diketonate complexes modulated by pH and proton flow

Materials Advances

ROYAL SOCIETY OF CHEMISTRY

COMMUNICATION

View Article Online
View Journal | View Issue

Cite this: *Mater. Adv.*, 2020, 1, 569

Received 22nd April 2020,
Accepted 2nd June 2020

DOI: 10.1039/d0ma00237b

rsc.li/materials-advances

Development of tuneable green-to-red emitting transparent film based on Nafion with Tb^{III}/Eu^{III} β-diketonate complexes modulated by pH and proton flow†

Hajime Kamebuchi, *[ab] Taiho Yoshioka[a] and Makoto Tadokoro *[a]

Nafion membranes are recognised as cation exchangers and excellent proton conductors. Emissive Ln^{III}-β-diketonate complexes, $[Ln^{III}_2(PBA)_6]$ (Ln = Eu, Tb; HPBA = *N*-(2-pyridinyl)benzoylacetamide), were incorporated into a transparent Nafion film. Upon incorporation, reversible emission by the green light emitter $[Tb^{III}_2(PBA)_6]$ and red light emitter $[Eu^{III}_2(PBA)_6]$ could be controlled through pH adjustment. $[Tb^{III}_2(PBA)_6]$ emitted only under acidic conditions, while $[Eu^{III}_2(PBA)_6]$ emitted only under basic conditions. Taking advantage of Nafion's high proton conductivity brought about dynamic changes in the wavelengths emitted by the film. When an in-plane external voltage was applied to the film, red wavelength emission appeared to migrate toward the negative electrode. Owing to the proton concentration gradient induced by the electric field, emission by Eu^{III} at 615 nm was enhanced near the positive electrode, whereas proton deficiency suppressed emission by $[Tb^{III}_2(PBA)_6]$. Tuneable emission in the transparent Nafion system enhances its potential for use as an energy-saving material.

Transparent luminescent materials that emit intensely under irradiation at specific wavelengths are highly promising energy-saving materials. These materials have potential for applications in light-emitting diodes (LEDs), displays and illuminators, because light scattering and self-absorption are reduced.[1] There are currently two ways to fabricate highly transparent and luminescent materials. Fluorescent nanoparticles can be incorporated, such as quantum dots,[2] which do not scatter visible light. Alternatively, luminescent ions, organic molecules and metal complexes can be dispersed in transparent glasses[3] or polymeric films.[4] The latter is a convenient way to produce luminescent materials with arbitrary sizes and shapes for emission at various wavelengths. However, it is difficult to control the emission wavelength in a single glass or film. It is also difficult to tune multicolour luminescence induced by external stimuli.

Tang *et al.* reported a multicolour-emitting transparent luminescent material with *N*-(2-pyridinyl)benzoylacetamide (HPBA) and lanthanide ions.[5] HPBA is a β-diketone compound containing an amide group and a pyridine ring.[5,6] Adding an amide group to β-diketonates would increase its triplet excitation energy, which would facilitate energy transfer from the ligand to the Tb^{III} core. In addition, the pyridine ring in HPBA enables emission wavelength modulation *via* pH adjustment, because changes to the S_1 and T_1 level of the β-diketonate ligand are caused by protonation and deprotonation. Therefore, HPBA is well-suited for materials in which luminescence is adjusted with changes in pH. It has been found that spin-coated poly(vinyl pyrrolidone) (PVP) films containing HPBA, Tb^{III} and Eu^{III} emit green light under acidic conditions, whereas red light is emitted by Eu^{III} ions under basic conditions.[5]

In this study, we employed Nafion as a solid medium for the fabrication of transparent luminescent materials with tuneable emissions. Nafion membranes are quite famous for their ability to conduct protons and exchange cations.[7] Nafion is composed of hydrophobic main chains and pendant hydrophilic side chains.[7c] The side chains are especially important. When Nafion is introduced to a polar solvent, solvent molecules are surrounded by side-chain sulfonic acid groups.[7b] Cavities ~4 nm in diameter form in Nafion when it is swollen with water or alcohol, and large molecules can be immobilised within them. Moreover, the proton conductivity of hydrated Nafion is very high and can reach up to 0.1 S cm^{-1}.[7d] A variety of functional films have been developed by using Nafion to take advantage of these properties.[8–16] This time, we first synthesised and crystallised the HPBA–Tb^{III} and HPBA–Eu^{III} complexes $[Tb^{III}_2(PBA)_6]$ (**1**) and $[Eu^{III}_2(PBA)_6]$ (**2**) as pH-sensitive emitters (Scheme 1). The complexes were easily incorporated into transparent Nafion film, and the excellent proton conduction in Nafion not only made it responsive to pH; the proton gradient within a $[Ln^{III}_2(PBA)_6]$@Nafion. We demonstrated a fine tuning

[a] *Department of Chemistry, Faculty of Science, Tokyo University of Science, Kagurazaka 1-3, Shinjuku-ku, Tokyo 162-8601, Japan*
[b] *Department of Chemistry, College of Humanities and Sciences, Nihon University, Sakurajosui 3-25-40, Setagaya-ku, Tokyo 156-8550, Japan. E-mail: hkame@chs.nihon-u.ac.jp*

† Electronic supplementary information (ESI) available: Detailed experimental procedures, tables for bond angles and distances, emission spectra in solution, and short movie about emission of the film under DC voltage. CCDC 1938544 and 1938545. For ESI and crystallographic data in CIF or other electronic format see DOI: 10.1039/d0ma00237b

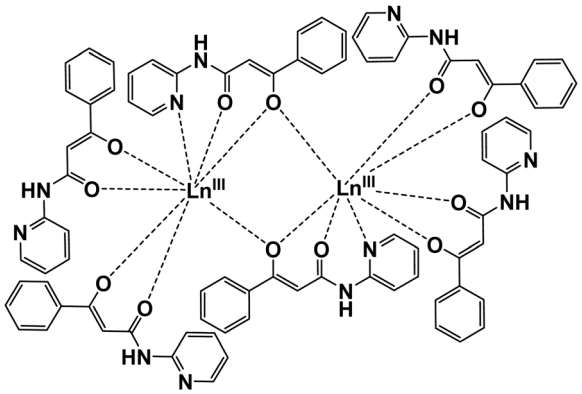

Scheme 1 Molecular structure of $[Ln^{III}_2(PBA)_6]$.

of emission colour in the transparent film by adjusting its pH with buffer solutions and manipulating the electric field.

HPBA was prepared with 2-aminopyridine and ethyl benzoylacetate in xylene according to a previously reported procedure.[17] **1** and **2** were synthesised and crystallised *via* slow diffusion of $Ln(NO_3)_3{\cdot}6H_2O$, HPBA and NaOH in MeOH. X-ray crystallographic analysis revealed unexpected dinuclear structures bridged by two PBA^- ligands, which are quite different molecular structures reported in ref. 11 and 12. Crystalline **1** and **2** were assigned to the orthorhombic *Pbca* space group. The crystallographic data, bond lengths, bond angles and hydrogen bonds of **1** and **2** are shown in Table 1 and Tables S1–S6 (ESI†). Formation of the isomorphous dinuclear complexes occurred through cross-linking of O(5) and O(5)* in the β-diketone group and N(5) in the pyridine moiety (Fig. 1 and Fig. S1, ESI†). Intermolecular hydrogen bonds formed between nitrogen atoms in the secondary amines (N(2), N(4)) and the uncoordinated pyridine groups (N(1), N(3)) on the four PBA^- ligands (Fig. S2 and S5, ESI†). Hydrogen bonds also formed between nitrogen atoms in the secondary amines of the bridging PBA^- ligands (N(6)) and H_2O (O(7)) as crystallisation water (Fig. S3 and S6, ESI†).

Table 1 Crystallographic data for compounds **1** and **2**

	1	**2**
Formula	$C_{84}H_{68}N_{12}O_{13}Tb_2$	$C_{84}H_{68}N_{12}O_{13}Eu_2$
Formula weight	1789.36	1775.44
Crystal system	Orthorhombic	Orthorhombic
Space group	*Pbca* (#61)	*Pbca* (#61)
a/Å	15.039(8)	15.0798(7)
b/Å	17.955(9)	17.9879(9)
c/Å	29.141(15)	29.0943(14)
V/Å^3	7869(7)	7891.9(7)
Z	4	4
T/K	173(2)	173(2)
d_{calc}/g cm^{-3}	1.510	1.494
μ(MoKα)/mm^{-1}	1.855	1.647
F(000)	3600	3584
Data	9735	9782
Parameters	513	513
R_1 [$I > 2\sigma(I)$]	0.0364	0.0344
wR_2 (all data)	0.0942	0.0767
G.O.F.	1.037	1.000
Differential peak/e Å^{-3}	1.647	1.181
Differential Hole/e Å^{-3}	−0.900	−0.637
CCDC	1938544	1938545

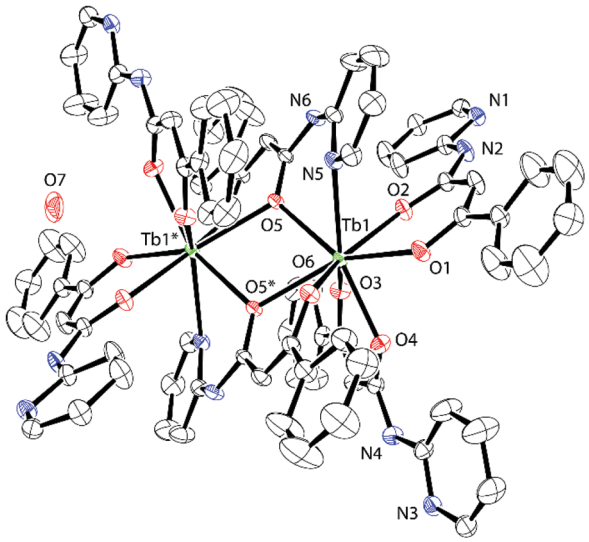

Fig. 1 ORTEP image of **1** with thermal ellipsoids at the 30% probability level.

The following hydrogen bond distances were observed in **1**: N(1)···N(4) = 3.013(5) Å; N(2)···N(3) = 3.031(5) Å; N(6)···O(7) = 2.913(5) Å. Fig. S4 and S7 (ESI†) show the coordination geometry around the Ln core. Six PBA^- ligands completed an 8-coordinated LnO_7N_1 core to form a rectangular prism. The top and bottom surfaces of the prism exhibited the so-called square antiprismatic geometry (SAP), in which they appeared twisted with respect to each other. The face-to-face distance in the SAP (d_{pp}), the minimum interatomic distance within each face (d_{in}) and the angles between the diagonals of the two faces (Φ) are shown in Fig. S4 (ESI†). The upper plane [O(1)O(2)O(3)O(4)] was a flat, nearly square rectangle with a d_{in} ranging from 2.719(4) to 2.761(4) Å. The lower plane [O(5)N(5)O(6)O(5)*] was a distorted rectangle with greater variation in d_{in}, which ranged from 2.778(4) to 3.330(5) Å. The angle Φ was 40.7(1)–50.1(2)°, while d_{pp} equalled 2.568(2) Å. In compound **2**, d_{in} in the [O(1)O(2)O(3)O(4)] plane ranged from 2.726(4) to 2.806(4) Å and from 2.785(3) to 3.413(4) Å in the [O(5)N(5)O(6)O(5)*] plane. Φ ranged from 40.4(1) to 51.2(1)°, and d_{pp} = 2.587(2) Å.

1 and **2** were readily introduced into Nafion due to its high cation exchange capacity. The treated Nafion film was referred to as **1**/**2**@Nafion. In contrast to methods like spin-coating and casting, the concentration of molecules absorbed by the Nafion film was not immediately distinct. We therefore needed to quantify the dinuclear lanthanide(III) complexes taken up by the film. We did so indirectly by continuously analysing the soaking solution with a UV-visible spectrometer. We then determined the relationship between complex absorption and time. We expected that after removing the film, the complex concentration in the soaking solution would be lower than it was before soaking the film. Consequently, peak intensity in the UV-vis absorption spectra of the soaking solution would decrease after adding the film. Changes in the absorption spectra thus enabled us to quantify the complexes taken up by **1**/**2**@Nafion. The dependence of the loading weight on

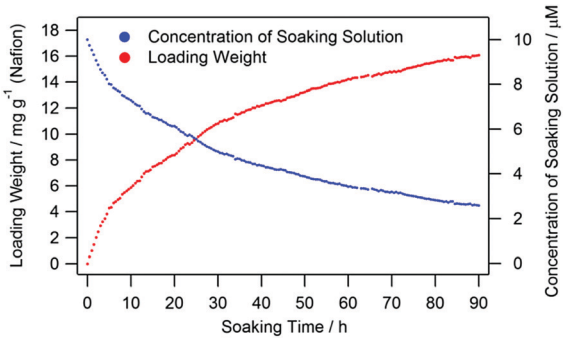

Fig. 2 The dependence of loading weight on soaking time (red). The concentration of the soaking solution is shown in blue.

soaking time estimated from the UV-vis spectra is shown in Fig. 2. The absorption peak intensity decreased with increasing soaking time. This decrease in intensity began to stabilise after 40 h of soaking. After 90 h, virtually no change in peak intensity was observed. The estimated complex concentration in **1**/**2**@Nafion was 16.08 mg g^{-1} (Table S7, ESI†).

Emission spectra of **1** and **2** in EtOH are shown in Fig. S8 (ESI†). The peaks at 545 and 615 nm originated from the $^5D_4 \rightarrow {}^7F_5$ and $^5D_0 \rightarrow {}^7F_2$ f–f transitions in Tb^{III} and Eu^{III}, respectively. **1** emitted green light, and emission was quenched under basic conditions. **2** emitted red light and was quenched under acidic conditions. Focusing on the emission spectrum of **2** here, the intensity of $^5D_0 \rightarrow {}^7F_2$ is about 7.7 times higher than that of $^5D_0 \rightarrow {}^7F_1$; $^5D_0 \rightarrow {}^7F_2$ is an electric dipole transition and is sensitive to site symmetry. Meanwhile, the $^5D_0 \rightarrow {}^7F_1$ transition is sensitive to the magnetic dipole effect and is actually not subject to the chemical surroundings of Eu^{III} ion. The large intensity ratio $I(^5D_0 \rightarrow {}^7F_2)/I(^5D_0 \rightarrow {}^7F_1)$ value for compound **2** reflects the low symmetry of the Eu^{III} ion as EuO_7N_1. For example, a homo-lanthanide 3D-framework, $\{[Eu^{III}(\mu_6\text{-ddpp})]\cdot H_2O\}_n$ (H_3ddpp = 2,5-di(2′,4′-dicarboxylpheny)pyridine acid), has a near-perfect SAP local symmetry of EuO_8, and its emission intensity ratio $I(^5D_0 \rightarrow {}^7F_2)/I(^5D_0 \rightarrow {}^7F_1)$ is about three.[18]

Incorporation of compounds **1** and **2** was carried out by soaking a plastic Nafion film in an EtOH solution that contained **1** and **2** in 1 : 1 molar ratio for 90 h at RT. The appearance and pH dependence of **1**/**2**@Nafion emission in Britton–Robinson buffer (BRB)[19] from pH 2 to 12 is shown in Fig. 3. When soaked in pH 2–5 solutions, **1**/**2**@Nafion emitted green light under UV irradiation at 365 nm. After soaking in pH 6–8 solutions, it emitted yellow light, while red light was emitted after soaking at pH 9–12. The peak at 615 nm in the emission spectra in Fig. 3 originating from Eu^{III} ($^5D_0 \rightarrow {}^7F_2$) became less intense as the pH decreased, while the peak at 545 nm originating from Tb^{III} ($^5D_4 \rightarrow {}^7F_5$) increased in intensity. Our observations supported the notion that the green light emitted by **1**/**2**@Nafion under acidic conditions originated from **1**, while the red light seen under basic conditions originated from **2**. The yellow light observed at pH 6–8 was likely a mixture of red and green light, since the peaks at 545 and 615 nm were both rather intense in the emission spectra. A relevant and important example is the fine tuning of

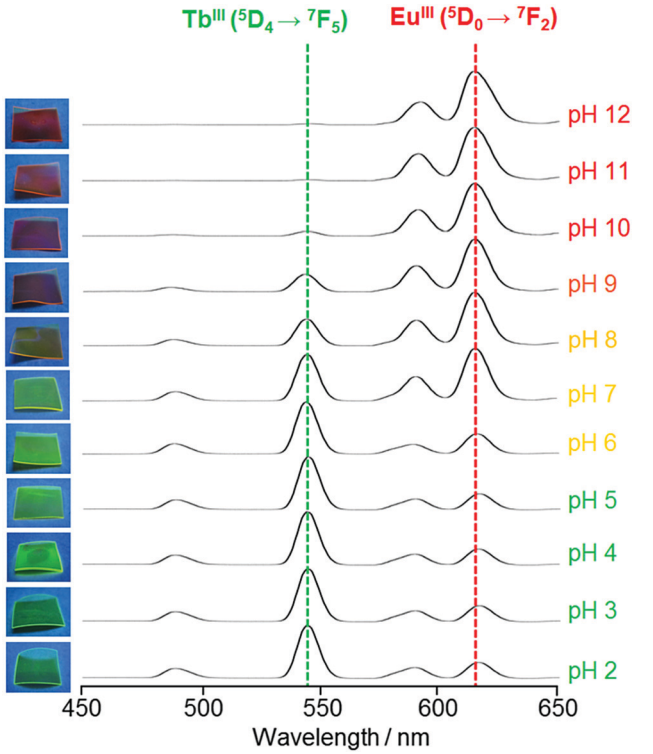

Fig. 3 Emission spectra showing pH dependence in **1**/**2**@Nafion. Pictures of the films at the corresponding pH values are shown on the left (λ_{ex} = 365 nm).

red to green emission in $\{[Eu_{3x}Tb_{3(1-x)}Zn_6(bipy)_2(Hmimda)_7]\cdot mH_2O\}_n$ (bipy = 4,4′-bipyridine, H_3mimda = 2-methyl-1-*H*-imidazole-4,5-dicarboxylic acid).[20] This is a functional material made up of carboxylate bridged Ln^{III} binuclear units with SAP local symmetry of LnO_8, where Hminda^{2-} and bipy are able to sensitise both Eu^{III} and Tb^{III} ions. It is demonstrated that the emission intensities of Tb^{III} $^5D_4 \rightarrow {}^7F_2$ and $^5D_4 \rightarrow {}^7F_5$ increase with increasing doping of Tb^{III} in this system, while the intensity of Eu^{III} $^5D_0 \rightarrow {}^7F_2$ gradually decreases. In the case of **1**/**2**@Nafion, on the other hand, the advantage is that the fine tuning of the luminescent colour can be done without changing the amount of lanthanide ions, because the pH was adjusted to determine whether the PBA$^-$ ligand sensitises Tb^{III} or Eu^{III} ions. Thus, **1**/**2**@Nafion has a potential application as an insightful pH sensor. A comparison with other reported examples in terms of sensor applications is that of a binary co-doped $Tb_{1-x}Eu_x$-tcptpy (H_3tcptpy = 4-(2,4,6-tricarboxylphenyl)-4,2′:6′,4″-terpyridine), which behaves as a luminescent thermometer.[21] This system has a SAP local symmetry of LnO_7N_1, and the intensity ratio $I(^5D_0 \rightarrow {}^7F_2)/I(^5D_0 \rightarrow {}^7F_1)$ is about 10.8 for Eu-tcptpy due to low site symmetry. In particular, $Tb_{0.897}Eu_{0.103}$-tcptpy with x = 0.103 exhibits the best temperature dependence of the emission, with a linear decrease of $^5D_4 \rightarrow {}^7F_5$ for Tb^{III} and a linear increase of $^5D_0 \rightarrow {}^7F_2$ for Eu^{III} in the range 305–340 K. As described above, functional materials that can precisely control the luminescence intensity of Tb^{III} and Eu^{III} have a variety of potential applications.

Since Nafion is a highly proton-conductive film, it is possible to create a proton concentration gradient through the membrane

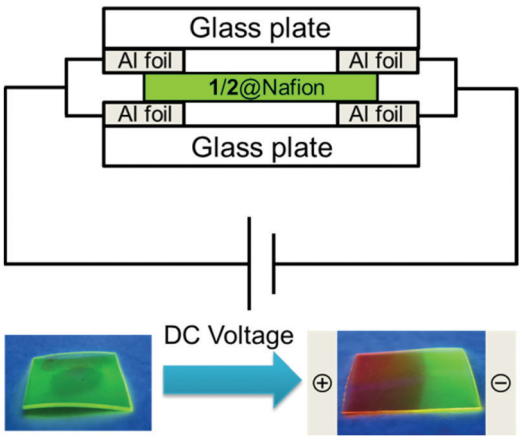

Fig. 4 Control of **1**/**2**@Nafion (pH 3) emission with proton flow under an applied voltage and irradiation with UV light (λ_{ex} = 365 nm).

by applying an external voltage. To take advantage of this property for control of **1**/**2**@Nafion emission, we manipulated the distribution of protons in the membrane by applying an external voltage. Before testing, **1**/**2**@Nafion was soaked in an acidic BRB solution (pH 3) for 5 min to ensure acidic conditions within the film. Voltage was applied through the film using the setup depicted in Fig. 4. Aluminium foil was attached to two glass slides. The film was held between the slides to ensure contact between it and the Al foil, and the setup was clamped in the upright position to secure the foil and film between the slides. Sandwiching the Nafion film between the glass slides also effectively prevented evaporation of water from the membrane.

A voltage of 40 V was then applied in plane using a SourceMeter® 2400 source measure unit (Keithley Instruments, USA). The in-plane distance between the electrodes was approximately 1 cm. Luminescence observations were performed by irradiating the films with 365 nm UV light while voltage was applied. Initially, **1**/**2**@Nafion emitted exclusively green light due to the protonation of **1** and **2** at pH 3. Red light emission was observed first at the positive electrode and gradually spread toward the negative electrode. After ~4 min, the entire film was emitting red light (Movie S1, ESI†). During the reaction, the film emitted green light around the negative electrode, red light around the positive electrode, and yellow light between the electrodes.

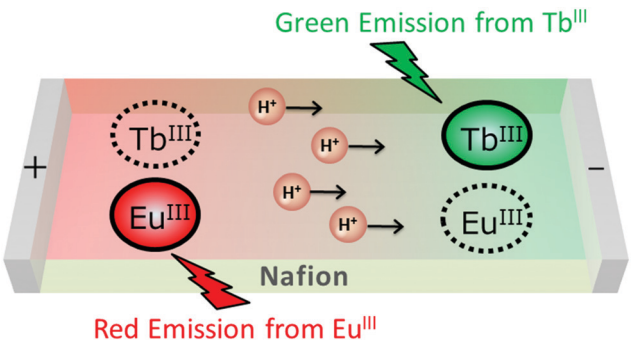

Fig. 5 Schematic illustration of **1**/**2**@Nafion emission tuning.

A conceptual diagram of the experiment is shown in Fig. 5. We could explain the observed phenomena in terms of proton distribution. The membrane was initially acidic, and emission of green light from Tb^{III} was predominant due to the abundance of protons in BRB at low pH. Protons migrated toward the negative electrode upon application of an external voltage. As the region around the positive electrode became deficient in protons, the deprotonated complexes became predominant. This suppressed emission by the Tb^{III} ion in **1**, and luminescence originating from the Eu^{III} ion in **2** was activated. This explained why the chromatic 'flow' appeared red to the naked eye.

Conclusions

The rationale for this study was the development of several functional transparent films by combining Nafion, a synthetic membrane that is well known for its ability to exchange cations and conduct protons, with functional metal complexes. When soaked in a solution of ionic metal complexes, the cation exchange capacity of Nafion enables spontaneous incorporation of the complexes. This tendency makes the preparation of transparent Nafion films with chromatic, magnetic, or luminescent properties originating in the incorporated molecules exceedingly simple. Most notably, it is possible to tune the functionality of films that contain proton-responsive complexes by applying a voltage through the membrane to induce proton flow. In this study, we controlled the luminescence of a Nafion film with pH and a proton concentration gradient induced by application of an external voltage. Since Nafion is transparent, incorporating luminescent complexes into Nafion films enables fabrication of transparent luminescent materials. Light scattering and self-absorption in the films are minimal, so they have potential for use as energy-saving materials. We are now adding a blue-light emitting complex to our system to fabricate a transparent material that emits light over the entire visible spectrum.

Conflicts of interest

The authors declare no competing financial interest.

Acknowledgements

H. K. kindly acknowledge funding by the Sasakawa Scientific Research Grant from The Japan Science Society (28-341), Tokyo Institute of Technology Foundation Research and Educational Grants (28-036), a research grant from The Mazda Foundation (16KK-354), a research grant from Izumi Science and Technology Foundation (H29-J-109), a research grant from Iketani Science and Technology Foundation (0301067-A).

References

1 (*a*) *Luminescent Materials and Applications*, ed. A. Kitai, Wiley, Chichester, 2008; (*b*) *Handbook of Luminescence, Display Materials and Devices*, ed. H. S. Nalwa and L. S. Rohwer, American Scientific Publishers, Valencia, 2003.

2 (*a*) S.-H. Shin, B. Hwang, Z.-J. Zhao, S. H. Jeon, J. Y. Jung, J.-H. Lee, B.-K. Ju and J.-H. Jeong, *Sci. Rep.*, 2018, **8**, 2463; (*b*) M. K. Choi, J. Yang and D.-H. Kim, *npj Flexible Electron.*, 2018, **2**, 10; (*c*) T. Frecker, D. Bailey, X. Arzeta-Ferrer, J. McBride and S. J. Rosenthal, *ECS J. Solid State Sci. Technol.*, 2016, **5**, R3019; (*d*) E. S. Shibu, M. Hamada, S. Nakanishi, S.-I. Wakida and V. Biju, *Coord. Chem. Rev.*, 2014, **263–264**, 2; (*e*) S. R. Alvarado, Y. Guo, T. P. A. Ruberu, E. Tavasoli and J. Vela, *Coord. Chem. Rev.*, 2014, **263–264**, 182; (*f*) H. Chen, L. Lin, H. Li and J.-M. Lin, *Coord. Chem. Rev.*, 2014, **263–264**, 86.

3 (*a*) C. Liu, B. Qian, R. Ni, X. Liu and J. Qiu, *RSC Adv.*, 2018, **8**, 31564; (*b*) M. Seshadri, V. de Carvalho dos Anjos and M. J. V. Bell, in *Luminescence: An Outlook on the Phenomena and their Applications*, ed. J. Thirumalai, IntechOpen, London, 2016.

4 (*a*) L. H. C. Francisco, M. C. F. C. Felinto, H. F. Brito, E. E. S. Teotonio and O. L. Malta, *J. Mater. Sci.: Mater. Electron.*, 2019, 1; (*b*) W. Li, P. Yan, G. Hou, H. Li and G. Li, *Dalton Trans.*, 2013, **42**, 11537; (*c*) J. Deschamps, A. Potdevin, N. Caperaa, G. Chadeyron, S. Therias and R. Mahiou, *New J. Chem.*, 2010, **34**, 385.

5 J. Xu, L. Jia, N. jin, Y. Ma, X. Liu, W. Wu, W. Liu, Y. Tang and F. Zhou, *Chem. – Eur. J.*, 2013, **19**, 4556.

6 X. Li, H. Chen, A. M. Kirillov, Y. Xie, C. Shan, B. Wang, C. Shi and Y. Tang, *Inorg. Chem. Front.*, 2016, **3**, 1014.

7 (*a*) K. Schmidt-Rohr and Q. Chen, *Nat. Mater.*, 2008, **7**, 75; (*b*) K. A. Mauritz and R. B. Moore, *Chem. Rev.*, 2004, **104**, 4535; (*c*) C. Heitner-Wirguin, *J. Membr. Sci.*, 1996, **120**, 1; (*d*) T. A. Zawodzinski Jr., M. Neeman, L. O. Sillerud and S. Gottesfeld, *J. Phys. Chem.*, 1991, **95**, 6040; (*e*) W. Y. Hsu and T. D. Gierke, *J. Membr. Sci.*, 1983, **13**, 307.

8 H. Kamebuchi, T. Jo, H. Shimizu, A. Okazawa, M. Enomoto and N. Kojima, *Chem. Lett.*, 2011, **40**, 888.

9 H. Kamebuchi, M. Enomoto and N. Kojima, in *Nafion: Properties, Structure and Applications*, ed. A. Sutton, Nova Science Publishers, New York, 2016, pp. 119–140.

10 (*a*) A. Nakamoto, H. Kamebuchi, M. Enomoto and N. Kojima, *Hyperfine Interact.*, 2012, **205**, 41; (*b*) A. Nakamoto, N. Kojima, L. X. Jun, Y. Moritomo and A. Nakamura, *Polyhedron*, 2005, **24**, 2909; (*c*) Y. Moritomo, Y. Isobe, X. J. Liu, T. Kawamoto, A. Nakamoto, N. Kojima, K. Kato and M. Takata, *J. Lumin.*, 2004, **108**, 229; (*d*) A. Nakamoto, Y. Ono, N. Kojima, D. Matsumura and T. Yokoyama, *Chem. Lett.*, 2003, **32**, 336; (*e*) N. Kojima, S. Toyazaki, M. Itoi, Y. Ono, W. Aoki, Y. Kobayashi, M. Seto and T. Yokoyama, *Mol. Cryst. Liq. Cryst.*, 2002, **376**, 567; (*f*) X. J. Liu, Y. Moritomo, A. Nakamura, T. Hirao, S. Toyazaki and N. Kojima, *J. Phys. Soc. Jpn.*, 2001, **70**, 2521.

11 (*a*) W. Kosaka, M. Tozawa, K. Hashimoto and S.-I. Ohkoshi, *Inorg. Chem. Commun.*, 2006, **9**, 920; (*b*) M. Tozawa, S.-I. Ohkoshi, N. Kojima and K. Hashimoto, *Chem. Commun.*, 2003, 1204.

12 (*a*) H. Hosokawa and T. Mochida, *Langmuir*, 2015, **31**, 13048; (*b*) H. Hosokawa, Y. Funasako and T. Mochida, *Chem. – Eur. J.*, 2014, **20**, 15014; (*c*) Y. Funasako and T. Mochida, *Chem. Commun.*, 2013, **49**, 4688.

13 Y. Funasako, A. Takaki, M. Inokuchi and T. Mochida, *Chem. Lett.*, 2016, **45**, 1397.

14 (*a*) Y. Zhuang and J. Zhang, *Luminescence*, 2010, **24**, 343; (*b*) Z. Cai, Z. Lin, X. Chen, T. Jia, P. Yu and X. Chen, *Luminescence*, 2010, **24**, 367; (*c*) M. N. Szentirmay, N. E. Prieto and C. R. Martin, *J. Phys. Chem.*, 1985, **89**, 3017; (*d*) N. E. Prieto and C. R. Martin, *J. Electrochem. Soc.*, 1984, **131**, 751.

15 (*a*) F. J. Sainz-Gonzalo, C. Popovici, M. Casimiro, A. Raya-Barón, F. López-Ortiz, I. Fernández, J. F. Fernández-Sánchez and A. Fernández-Gutiérrez, *Analyst*, 2013, **138**, 6134; (*b*) S. M. Shilov, K. A. Gavronskaya, A. N. Borisov and V. N. Pak, *Russ. J. Gen. Chem.*, 2008, **78**, 1775; (*c*) A. A. Petushkov, S. M. Shirov, M. V. Puzyk and V. N. Pak, *Russ. J. Phys. Chem. A*, 2007, **81**, 612; (*d*) A. A. Petushkov, S. M. Shilov and V. N. Pak, *J. Lumin.*, 2006, **116**, 127.

16 (*a*) H. Dacres and R. Narayanaswamy, *Sens. Actuators, B*, 2005, **107**, 14; (*b*) A. G. Ryder, S. Power and T. J. Glynn, *Appl. Spectrosc.*, 2003, **57**, 73; (*c*) C.-M. Chan, W. Lo and K.-Y. Wong, *Biosens. Bioelectron.*, 2000, **15**, 7; (*d*) D. García-Fresnadillo, M. D. Marazuela, M. C. Moreno-Bondi and G. Orellana, *Langmuir*, 1999, **15**, 6451; (*e*) C.-M. Chan, C.-S. Fung, K.-Y. Wong and W. Lo, *Analyst*, 1998, **123**, 1843.

17 B. Zaleska, B. Trzewik, E. Stodolak, J. Grochowski and P. Serda, *Synthesis*, 2004, 2975.

18 X. Feng, R. Li, L. Wang, S.-W. Ng, G. Qin and L. Ma, *CrystEngComm*, 2015, **17**, 7878.

19 H. T. S. Britton and R. A. Robinson, *J. Chem. Soc.*, 1931, 1456.

20 X. Feng, Y. Feng, N. Guo, Y. Sun, T. Zhang, L. Ma and L. Wang, *Inorg. Chem.*, 2017, **56**, 1713.

21 X. Feng, Y. Shang, H. Zhang, X. Liu, X. Wang, N. Chen, L. Wang and Z. Li, *Dalton Trans.*, 2020, **49**, 4741.